GEOPHYSICAL RESEARCH LETTERS, VOL. 28, NO. 24, PAGES 4531-4534, DECEMBER 15, 2001

The existence of a tertiary ozone maximum in the high-latitude middle mesosphere

Daniel Marsh and Anne Smith

National Center for Atmospheric Research, Boulder, Colorado

Guy Brasseur

Max Planck Institute for Meteorology, Hamburg, Germany.

Martin Kaufmann and Klaus Grossmann

Department of Physics, Wuppertal University, Wuppertal, Germany.

Abstract. Modeling and observations provide evidence of the existence of a tertiary ozone maximum in the middle mesosphere restricted to winter high-latitudes. This local maximum occurs at approximately 72 km altitude, at latitudes just equatorward of the polar night terminator. Model analysis indicates that this maximum is the result of a decrease in atomic oxygen losses by catalytic cycles involving the odd-hydrogen species OH and HO_2. In the middle mesosphere, at high latitudes, the atmosphere becomes optically thick to ultra-violet radiation at wavelengths below 185 nm. Since photolysis of water vapor is the primary source of odd-hydrogen, reduced ultra-violet radiation results in less odd-hydrogen and consequently lower oxygen loss rates. The consequent increase in atomic oxygen results in higher ozone because atomic oxygen recombination remains the only significant source of ozone in the mesosphere.

Introduction

Chapman first proposed a chemical scheme that describes the distribution of ozone in the terrestrial atmosphere [*Chapman,* 1930]. His simple scheme, based solely on a chemistry of oxygen species correctly predicted the existence of a stratospheric ozone layer. Although the exact height and magnitude of the layer has been modified by the inclusion of other reactions, the only significant source of ozone in the stratosphere remains the two-step process resulting from the absorption of ultra-violet (u.v.) radiation in the Herzberg continuum (185 to 242 nm):

$$O_2 + h\nu \rightarrow O + O \quad (1)$$

$$O + O_2 + M \rightarrow O_3 + M, \quad (2)$$

where M is a "third body", i.e. molecular nitrogen or oxygen. Observations and models show that the maximum stratospheric ozone mixing ratios are located between 30 and 35 km in the tropics.

The presence of a "secondary maximum", near the mesopause, was detected by *Hays and Roble* [1973] using satellite based stellar occultation observations. Here, again, the ozone peak is the result of radiation absorption but at shorter wavelengths in the Schumann Runge system (137 to 200 nm). The depth of the minimum between these layers depends on the destruction rates of atomic oxygen and ozone by odd-hydrogen species ($HO_x = H + OH + HO_2$) that act in catalytic cycles [*Bates and Nicolet,* 1950]. In this letter, we show that there exists a third or "tertiary" ozone maximum in the middle mesosphere that is restricted to latitudes near the polar night terminator. This maximum is clearly seen in both observations and models and is produced when ozone losses through catalytic cycles that involve hydrogen compounds are reduced because of a reduction in u.v. photolysis of water vapor.

Paper number 2001GL013791.
0094-8276/01/2001GL013791$05.00

Observations

To date there have been relatively few nighttime observations of ozone in the mesosphere. Historically most mesospheric ozone climatologies are based on daytime measurements because the observational technique requires either solar occultation or the presence of photolysis (see e.g. *Keating et al.* [1996]). We present nighttime observations from two instruments that observe ozone thermal emissions.

The CRyogenic Infrared Spectrometers and Telescopes for the Atmosphere (CRISTA) instrument was flown as part of the Shuttle Palette Satellite on two occasions: November 4 through 12, 1994, and August 8 through 16, 1997 [*Offermann et al.,* 1999]. Its primary purpose is the study of small and medium scale dynamics seen in atmospheric constituents. Recently, observations of the 9.6 μm band of ozone have been used to derive ozone densities up to 90 km. Figure 1 shows averages of ozone profiles from the second CRISTA flight. Data shown are from August 13 to 15, during which time CRISTA observed up to a latitude of 70°S. All profiles show increasing ozone mixing ratios above 80 km, where the lower part of the secondary maximum is observed. Below this altitude, equatorial and mid-latitude profiles are remarkably similar, while there exists a distinct ozone layer centered at 72.5 km in the high-latitude profile that is not present in the lower latitude profiles. The presence of this high-latitude ozone layer cannot be attributed to inaccuracies in the temperatures used in the retrieval. Ozone derivations use co-located CRISTA temperature measurements [*Riese et al.*, 1999], which at the height of the layer are reported to have an accuracy of ±2 K.

For comparison, we show nighttime ozone measurements in the mesosphere made by the Microwave Limb Sounder

(MLS) on board the Upper Atmosphere Research Satellite [*Froidevaux et al.,* 1996]. Figure 2 shows ozone mixing ratios derived from MLS 183 GHz radiometer (version 5) measurements during August, when MLS viewed the high-latitude Southern hemisphere. Again ozone mixing ratios in the tropics (2°S and 30°S) are remarkably similar, while the high-latitude ozone profile shows a local maximum in excess of 2.5 ppmv around 75 km. Differences in the size of the maximum are likely due to the fact that MLS data are taken at a higher latitude than the CRISTA data. Analysis of data from February 1992 (not shown) show a similar peak at 75°N, which indicates that this phenomenon is not restricted to the Southern hemisphere.

Modeling

A middle mesospheric tertiary maximum in ozone has been modeled in both two- and three-dimensional models. For example, the two-dimensional model of *Brasseur et al.* [2000] shows a local maximum in zonal mean ozone mixing ratios near 70 km, at 65°N latitude during January. Here, we show results from ROSE, a global 3-dimensional mechanistic chemical dynamical model based on the model developed by *Rose* [1983] and *Rose and Brasseur* [1989]. The model is typically run with a resolution of 5° in latitude, 11.25° in longitude and 2.5 km in altitude. Currently, the altitude range of the model is 17.5 km to 110 km. ROSE incorporates chemistry for 27 species, including reactions important for odd-oxygen (O_x = O + O_3) and odd-hydrogen, as well as chlorine and nitrogen chemistry. Where available, reaction rates are based on the current JPL compilation [*Sander et al.,* 2000].

Shown in Figure 3 are ozone predictions for August 15 at midnight local time. The model predicts a stratospheric ozone maximum near 10-11 parts per million by volume (ppmv) at approximately 32 km altitude. In addition, the ozone secondary maximum is also modeled, centered around 97.5 km in altitude. Between 70 and 80 km there is a distinct local maximum in ozone at 72.5°S latitude, where mixing ratios reach 7.9 ppmv. This local maximum is a robust feature of the model simulations, and occurs irrespective of changes to the chemical solver, transport or photolysis scheme. While the latitude and altitude of the maximum appear to be in good agreement with observations, the model peak amplitude is more than double that determined from the available observations. One possible reason for this discrepancy is that the satellite observations may not provide the high vertical resolution required to resolve the peak concentration.

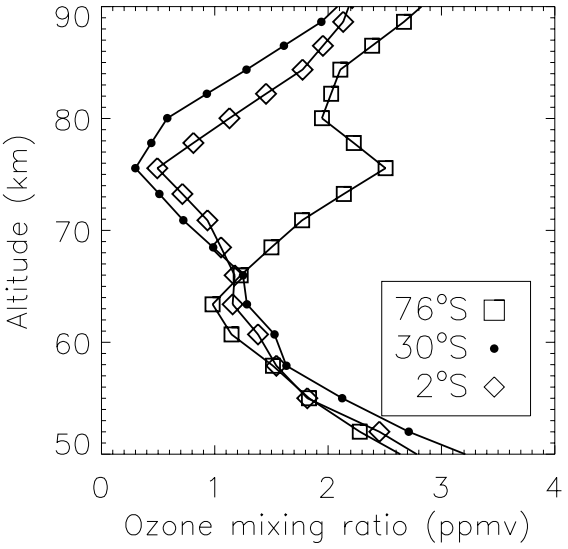

Figure 2. Mean mesospheric profiles of MLS 183 GHz radiometer ozone measurements taken between August 16 and 21 , 1992. Approximate local times of observations are 2035, 2350, and 0049 hours at 76°S, 30°S, and 2°S respectively. Between 52 and 63 profiles are included in each mean profile.

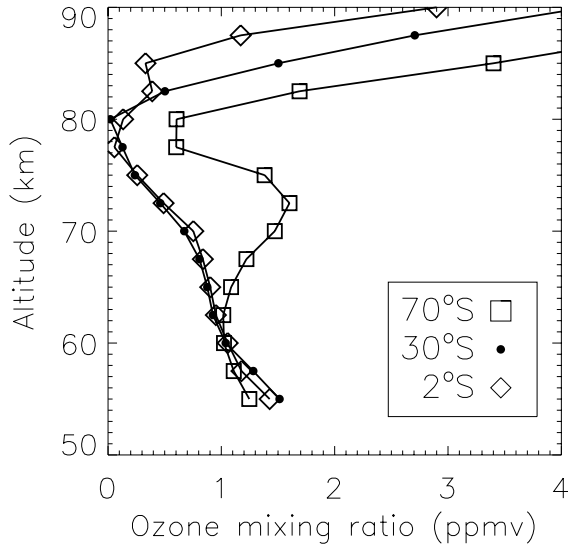

Figure 1. CRISTA 2 observations of mesospheric ozone mixing ratio (ppmv) at three different latitudes. Data are averages of profiles taken between August 13 and 15, 1997. Local times are approximately midnight, 0400 and 0500 hours for 70°S, 30°S and 2°S respectively.

To provide insight into the cause of the tertiary ozone maximum, southern hemisphere polar views of model odd-oxygen and OH at 72.5 km are depicted in Figure 4. Odd-oxygen mixing ratios are at a maximum (>10 ppmv) poleward of 60°S, but outside the polar night region. This indicates that the tertiary maximum in ozone is a reflection of increased odd-oxygen, i.e. the large nighttime ozone mixing ratios seen at high-latitudes are not merely caused by a re-partitioning of the available odd-oxygen. The polar plots show that both O_x and OH concentrations increase at low- and mid-latitudes beginning after sunrise, due respectively to the onset of molecular oxygen photolysis (primarily in the Schumann-Runge bands) and water vapor photolysis (primarily at Lyman-α). In this altitude region, odd-oxygen loss rates are dominated by the following catalytic cycle:

$$O + OH \rightarrow O_2 + H \quad (3)$$

$$H + O_2 + M \rightarrow HO_2 + M \quad (4)$$

$$O + HO_2 \rightarrow O_2 + OH. \quad (5)$$

Therefore, as OH concentrations increase in the afternoon due to water vapor photolysis, the odd-oxygen concentrations decrease. However, near the polar night terminator

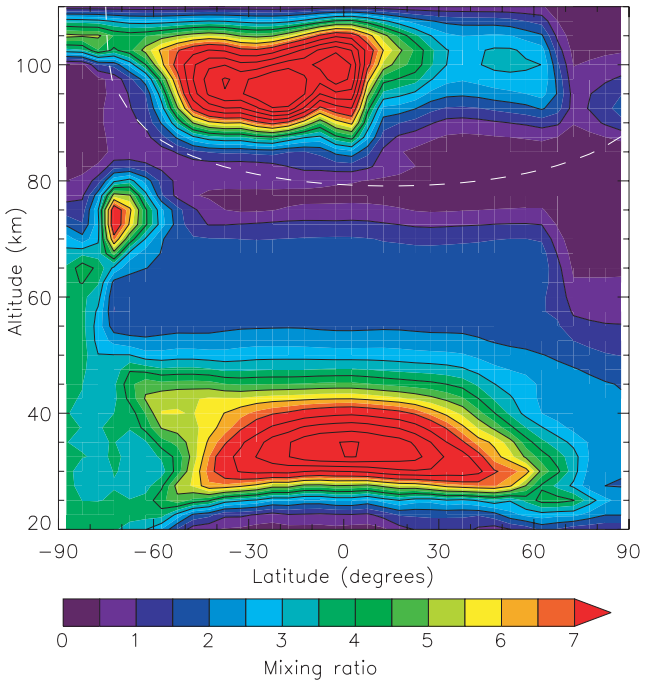

Figure 3. ROSE modeled ozone mixing ratio (ppmv) for August 15 at midnight local time. Dashed line indicates altitude at which noontime water vapor photolysis rates drop to 1/e of their maximum.

there is little OH production due to the attenuation of solar radiation below 185 nm and the subsequent absence of water vapor photolysis. The approximate height at which water vapor photolysis rates are reduced by a factor of 1/e of the noontime maximum is shown as a dashed line in Figure 3. It clearly shows that, at high-latitudes, there is a significant reduction in water vapor photolysis rates at altitudes above the ozone tertiary maximum. However, radiation in the Schumann-Runge bands and Herzberg continuum (between 185 and 242 nm) continues to penetrate to high-latitudes and so odd-oxygen is still produced through O_2 photolysis. Consequently, without OH losses, odd-oxygen concentrations continue to increase throughout the day, and persist throughout the night as is evident from the annulus of odd-oxygen centered near 70°S in Figure 4a.

Figure 5 shows the evolution over 24 hours of the photochemical production and loss of O_x at 72.5 km during winter at 2.5° and 67.5° latitude, respectively. As expected, this net production is equal to zero during nighttime. At sunrise, the photolysis of O_2 starts producing oxygen atoms (and ozone molecules), while the O_x loss remains small, since the availability of odd-hydrogen radicals at 70-75 km (see eqs. 3-5) by water vapor photolysis remains limited for high solar zenith angles. As a result, at all latitudes, the net odd-oxygen source is positive in the early morning, and the concentration of ozone increases with time.

At 2.5°S latitude, as time progresses and the Sun's elevation becomes larger, water photolysis is enhanced and the concentration of OH increases. Consequently, the net odd-oxygen production decreases, and even becomes negative after 10 am. In the afternoon, as the concentration of photochemically produced odd-hydrogen decreases with decreasing solar elevation, the O_x loss rates decrease, and near sunset, the net source becomes close to zero. In contrast, at 67.5°S, after the initial rise in O_x production, the net production remains positive throughout the day because the concentration of OH remains small during daytime. In both cases, just after sunset, there is a brief increase in O_x loss rates due to the rapid conversion of atomic oxygen to ozone and the consequent loss through the following reaction:

$$H + O_3 \rightarrow OH + O_2. \quad (6)$$

As atomic hydrogen is rapidly converted to OH after sunset (clearly seen in Figure 4b), the effectiveness of this loss channel decreases over a few hours.

The tropical and high-latitude net odd-oxygen sources at 72.5 km integrated over 24 hours are both small (nearly photochemical equilibrium conditions). In this situation, the equilibrium value for odd-oxygen is approximately the ratio of mean production to mean loss. Odd-oxygen values at high latitudes are higher than at the tropics because the ratio of production to loss for odd-oxygen is much larger at high-latitudes, and therefore the equilibrium value will be much higher.

The tertiary maximum is not seen near the stratopause because in this region the main source of odd-hydrogen is the reaction of water vapor with excited atomic oxygen ($O(^1D)$) and not u.v. photolysis. The primary source of

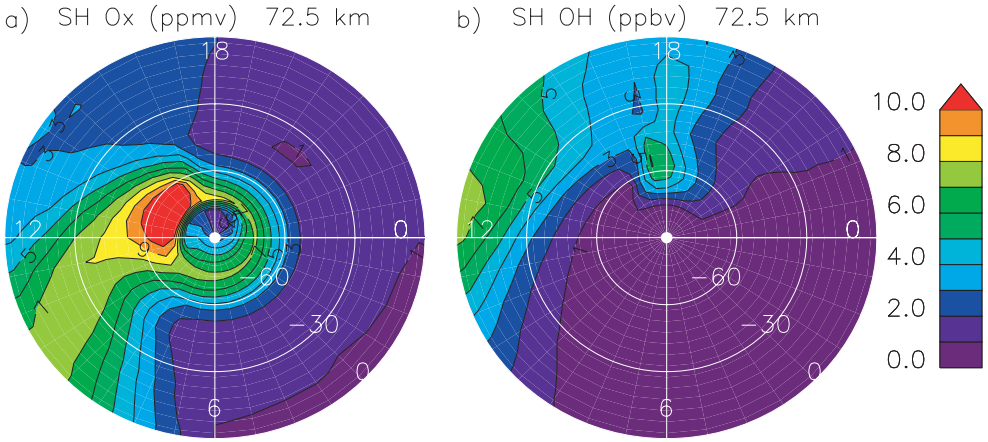

Figure 4. Southern hemisphere polar projections of ROSE modeled volume mixing ratios for (a) odd-oxygen and (b) OH on August 15 at 72.5 km. Contour intervals 1 ppmv for odd-oxygen and 1 ppbv for OH. Local times increase clockwise from the right.

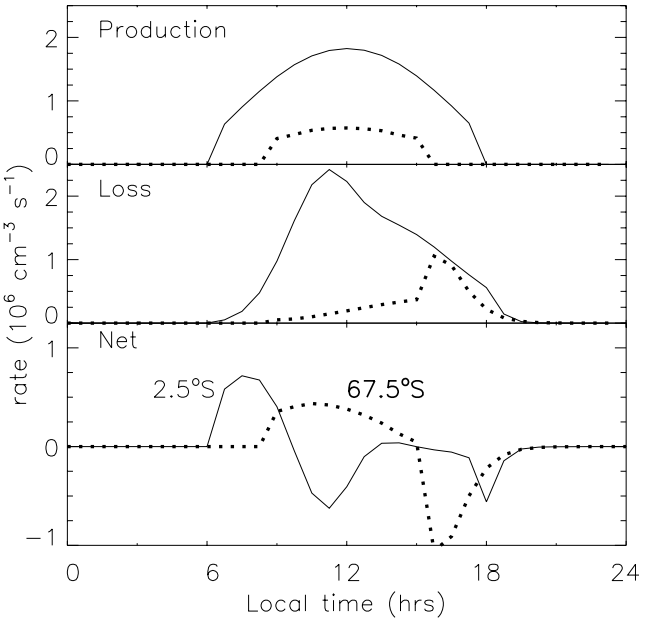

Figure 5. ROSE model odd-oxygen production and loss rates (10^6 molecules cm^{-3} s^{-1}) over 24 hours at 72.5 km. Data shown are for August 15 for 2.5°S (solid line) and 72.5°S (dashed line) latitude.

$O(^1D)$ is ozone photolysis at wavelengths shortward of 310 nm. The atmosphere is optically thin in this spectral range, and so HO_x production occurs near the polar night terminator. This is unlike the case at higher altitudes, where HO_x production is diminished near the terminator. In addition, any local maximum in ozone would result in more $O(^1D)$, and consequently more odd-hydrogen, thus providing a negative feedback.

Summary

Recent satellite observations reveal the existence of a local maximum in mesospheric ozone mixing ratios near 72 km, that occurs only in the wintertime hemisphere at high-latitudes. Modeling using a 3-dimensional chemical transport model reveals that the maximum is caused by low concentrations of odd-hydrogen and the subsequent decrease in odd-oxygen losses through catalytic cycles involving hydroxyl. These low concentrations are caused by diminished water vapor photolysis rates - the result of solar radiation at wavelengths below 185 nm being sharply attenuated by the large optical depths at high latitudes. On the other hand, odd-oxygen continues to be produced by O_2 photolysis by radiation at longer wavelengths which is not attenuated as sharply. Therefore, the local maximum is caused by a relatively large decrease in destruction, not matched by a decrease in production.

While models and data agree on the position of the maximum, there appears to be a discrepancy between model predictions and observations of the peak mixing ratio at the tertiary maximum. It may be that ozone observations made by the Thermosphere Ionosphere Mesosphere Energetics and Dynamics satellite (whose orbit has good coverage of the polar regions) will provide a long term characterization of the tertiary maximum, and allow resolution of this discrepancy.

Acknowledgments. The work of M. Kaufmann is partially supported by GSF, Forschungszentrum für Umwelt und Gesundheit GmbH, grant 07ATF10.

References

Bates, D.R., and M. Nicolet, Atmospheric hydrogen, *Publ. Astron. Soc. Pacific,* 62, 106, 1950.

Brasseur, G.P., A.K. Smith, R. Khosravi, T. Huang, S. Walters et al., Natural and human-induced perturbations in the middle atmosphere: a short tutorial, Atmospheric Science Across the Stratopause, Geophysical Monograph 123, 7-20, AGU, 2000.

Chapman, S., On ozone and atomic oxygen in the upper atmosphere, *Phil. Mag. S.*, 7, 369-383, 1930.

Froidevaux, L., W.G. Read, T.A. Lungu, R.E. Cofield, E.F. Fishbein, et al., Validation of UARS Microwave Limb Sounder ozone measurements, *J. Geophys. Res.,* 101, 10,017-10,060, 1996.

Hays, P.B., and R.G. Roble, Observation of mesospheric ozone at low latitudes, *Planet. Space Sci.,* 21, 273-279, 1973.

Keating, G.M., L.S. Chiou, and N.C. Hsu, Improved ozone reference models for the COSPAR international reference atmosphere, *Adv. Space Res.*, 18, (9/10)11-58, 1996.

Offermann, D., K.U. Grossmann, P. Barthol, P. Knieling, M. Riese, and R. Trant, The CRyogenic Infrared Spectrometers and Telescopes for the Atmosphere (CRISTA) experiment and middle atmosphere variability, *J. Geophys. Res.,* 104, 16,311-16,325, 1999.

Riese, M., R. Spang, P. Preusse, M. Ern, M. Jarisch, et al., Cryogenic Infrared Spectrometers and Telescopes for the Atmosphere (CRISTA) data processing and atmospheric temperature and trace gas retrieval, *J. Geophys. Res.,* 104, 16349-16347, 1999.

Rose, K., On the influence on nonlinear wave-wave interactions in a 3-d primitive equation model for sudden stratospheric warmings, *Beitr. Phys. Atmosph.,* 56, 14-41, 1983.

Rose, K., and G.Brasseur, A three-dimensional model of chemically active trace species in the middle atmosphere during disturbed winter conditions, *J. Geophys. Res.,* 94, 16,387-16,403, 1989.

S.P. Sander, R.R. Friedl, DeMore, W.B., D.M. Golden, M.J.Kurylo, et al., Chemical kinetics and photochemical data for use in stratospheric modeling, Supplement to Evaluation 12: Update of key reactions, Evaluation number 13, JPL Publ., 00-3, 2000.

D.R. Marsh, A.K. Smith, National Center for Atmospheric Research, P.O. Box 3000, Boulder, CO 80307-3000. (email: marsh@ucar.edu, aksmith@ucar.edu)

G.P. Brasseur, Max Planck Institute for Meteorology, 20146 Hamburg, Germany. (email: brasseur@dkrz.de)

M. Kaufmann, K.U. Grossmann, Department of Physics, Wuppertal University, D-42119 Wuppertal, Germany. (email: kaufmann@wpos2.physik.uni-wuppertal.de)

(Received July 18, 2001; revised October 1, 2001; accepted October 3, 2001.)